*XVII IMEKO World Congress*
*Metrology in the 3rd Millennium*
*June 22–27, 2003, Dubrovnik, Croatia*

# AUTOMATIC PAPILLA SHAPE DETECTION IN STEREO RETINAL IMAGES BASED ON IMAGE FUSION FOR COMPUTER AIDED GLAUCOMA DIAGNOSTICS

*Yandong Tang, Axel von Freyberg, Horst Selzer, Gert Goch*

Bremen Institute of Industrial Technology and Applied Work Science (BIBA) at the University of Bremen, Bremen, Germany

**Abstract –** This paper presents a number of image processing methods, including the fusion method, for analysing digitised fundus images. For computer aided Glaucoma diagnostics it is necessary to robustly and automatically detect the main regions (e.g. the papilla) within an image. This represents a major challenge, since a broad variety of images taken in different clinics with different cameras exist. For this purpose adapted methods are actually developed in the EU-project GlauCAD (Glaucoma Prevention by Computer Aided Diagnostics).

Keywords: image processing, glaucoma

## 1. INTRODUCTION

With the advancement of medical imaging and computer vision technology, the effective use of image-guided diagnostics and treatment has been a focus of research in image processing and computer vision. The employment of digital fundus imaging provides ophthalmologists with digitised data that could be exploited for computerised detection of eye disease based on image processing and pattern recognition technology [1].

For the diagnosis of eye diseases, such as glaucoma, the ophthalmologists concentrate on the area around the papilla and pay most of their attention to changes in this region (see Fig. 1). Therefore, both the identification and the shape analysis of the papilla in fundus images are very important for the detection of glaucoma at an early stage. The methods to be presented are necessary to automatically calculate feature parameters, such as disc radius, cup radius and shape variations of the papilla within a sequence of fundus images of one eye. By these quantitative features the early detection and grading of glaucoma might be greatly facilitated.

Due to very different exposure conditions and qualities of more than 16000 fundus images in the database resulting from the European Glaucoma Prevention Study, some published effective methods of papilla detection in [2][3][5] were tested and found to fail due to a low accurate rate of papilla detection. These methods either used one colour channel (red, green or grey), or are effective only for low resolution fundus images, and were not tested on large numbers of fundus images with varying qualities.

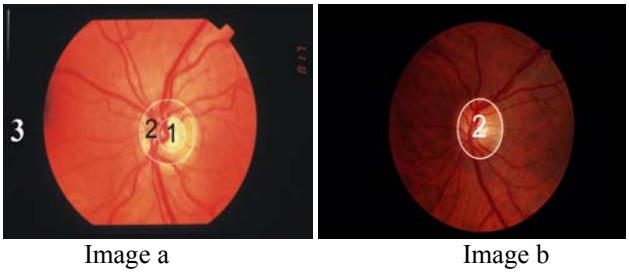


Image a Image b

Fig. 1. Two fundus images. Zone 1 represents the cup, Zone 2 is the optic disc (papilla), Zone 3 is the black mask area.

Image fusion refers to the technology that integrates complementation information from multi-image data such that the new images are more suitable for the purpose of human visual perception and the computer processing tasks such as feature extraction and object recognition [4]. In this paper the papilla is recognised by the red channel, the green channel and the variance image respectively. As each of the three partial results is only effective to one kind of image or contains only parts of the papilla, the fusion of these results is used for a more accurate detection of the papilla. As outlined in the following sections, a convenient postprocessing of the fusion result effectively detects the papilla within a fundus image.

## 2. AUTOMATIC SHAPE DETECTION METHOD OF THE PAPILLA IN FUNDUS IMAGES

In colour fundus images the papilla appears as a bright or yellowish region (see Fig. 1). Its shape appears more or less as a circle or an ellipse. Its size varies from image to image. In the fundus image database of the European Glaucoma Prevention Study the diameter of the papilla is not larger than 800 pixels in fundus images obtained with a resolution of 4032x2688 pixels.

### *2.1. Locating the centre of the papilla in fundus images and pre-processing of the fundus image*

In [2] the papilla centre is localised using high grey level variation. It is the pixel point in the variance image, which has the absolute grey maximum value. This approach has proved to work very well, if there are no or few pathologies like exudates or some noise, that appear also very bright and are also well contrasted [6]. Therefore, the papilla centre in fundus images is characterised in some cases only by a local grey value maximum. For locating the centre in a fundus image by its variance image, a simple area threshold is

applied to obtain a binary image ***Vb*** from the variance image. The local maximum pixel point that is located in the largest part in the binary image ***Vb*** and that is furthermost from the image boundary, marks the papilla centre (see Fig. 2). Fig. 2 shows two examples of variance images and the detected centres of the papillae.

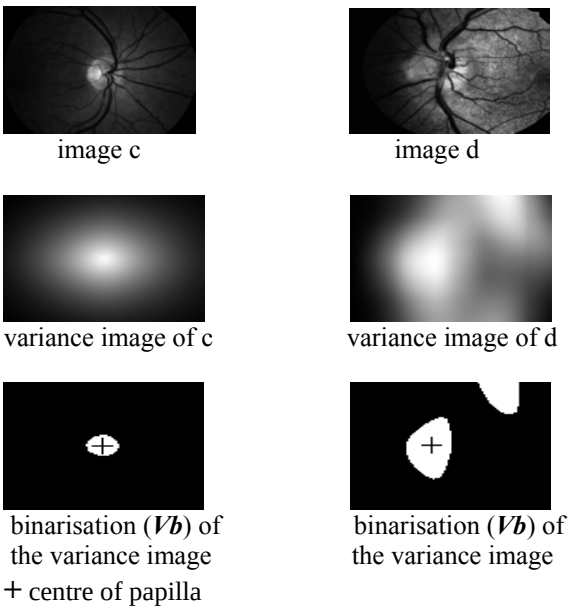


Fig.2 Two examples of papilla locating within a fundus image

*2.2. Automatic papilla detection with the red and green channels and the variance image respectively*

Most of the papers about automatic papilla detection with different methods, such as Hough transform [5], mathematical morphology [6] and neural networks used only the red intensity to detect the contour usually in low resolution (about 600x400 pixels) and their algorithms were tested with few samples. For processing a large amount of fundus images in the database resulting from the European Glaucoma Prevention Study with very different exposure conditions, qualities and higher resolution images (about 4032x2688 pixels, 48 bit RGB), in [3] a method with binarisation of the red colour channel by means of an adaptive threshold and linear gradient compensation approach is presented. Tests with different kinds of images from the database showed that the red intensity indicates the border of the papilla plainest for about 60% of more than 300 fundus images tested, and that for more than 30 % of them the green intensity shows the distinct area of the papilla. Compared to red and green, the blue channel shows no distinct area. Experience showed that with one colour intensity of a fundus image it is very difficult to detect the papilla with higher accuracy for all kinds of fundus images in the database. As it is very difficult to identify in advance which colour channel will deliver the best result, the fusion strategy is used by a combination of papilla detections with the red and green components in RGB colour model, the intensity component in HIS (hue, saturation, and intensity) colour model and the variance (measurement for the contrast within adjacent pixels) of a fundus image.

Let $\boldsymbol{R}(x,y)$, $\boldsymbol{G}(x,y)$, $\boldsymbol{B}(x,y)$ and $\boldsymbol{Q}(x,y)$ be respectively the intensity functions of the red, green and blue channels and of the variance image. $\boldsymbol{T}(x,y)$ is the intensity function of the original image in HSI model. For convenience $\boldsymbol{I}$ is denoted as the set of pixel points of a fundus image. The papilla detected in the fundus image by each channel (red, green and intensity in HSI) with the method presented in [3] is denoted respectively as binary images:

$$\boldsymbol{R_b(x,y)}, \boldsymbol{G_b(x,y)} \text{ and } \boldsymbol{T_b(x,y)}.$$

In these binary images a pixel point $(x,y)\in\boldsymbol{I}$, whose value is 1 (white pixel point), is denoted in the papilla region. All pixel points with value 1 in one of these three binary images are candidates for pixel points in the papilla in fusion strategy. The variance image $\boldsymbol{Q}$ is transformed into $\boldsymbol{Q'}$ to change the local maximum intensity of the papilla centre to an absolute maximum for correct generation of two mask images used in the papilla recognition.

$$\boldsymbol{Q'(x,y)} = \boldsymbol{Q(x,y)} \times \boldsymbol{e}^{-\sqrt{\frac{(x-x_c)^2+\ (y-y_c)^2}{\omega}}} \qquad (1)$$

here $(\boldsymbol{x_c}, \boldsymbol{y_c})$ is the location of the papilla centre, $\boldsymbol{\omega}$ is the maximum distance from the point $(\boldsymbol{x_c}, \boldsymbol{y_c})$ to the boundary of $\boldsymbol{I}$, $(x, y)\in\boldsymbol{I}$ and $\boldsymbol{Q'}$ $(x,y)$ is the normalised variance image as $0\le\boldsymbol{Q'}(x,y)\le 1$.

The two masks for the papilla recognition are defined as:

$$\boldsymbol{q_1(x,y)} = \begin{cases} 1 & \boldsymbol{Q'(x,y)} > \boldsymbol{Th_1} \\ 0 & \boldsymbol{Q'(x,y)} \le \boldsymbol{Th_1} \end{cases} \qquad (2)$$

$$\boldsymbol{q_2(x,y)} = \begin{cases} 1 & \boldsymbol{Q'(x,y)} > \boldsymbol{Th_2} \\ 0 & \boldsymbol{Q'(x,y)} \le \boldsymbol{Th_2} \end{cases} \qquad (3)$$

Here the two threshold values $\boldsymbol{Th_1}$ =0.26 and $\boldsymbol{Th_2}$ =0.45 are determined by statistics.

The region of a set $\overline{\boldsymbol{q}}_1$ ={(x,y) | (x,y) $\in\boldsymbol{I}$ and $\boldsymbol{q_1}$ (x,y)=1} is larger than the papilla and contains the papilla region. The region $\overline{\boldsymbol{q}}_2$ ={(x,y) | (x,y) $\in\boldsymbol{I}$ and $\boldsymbol{q_2}$ (x,y)=1} is contained in the papilla and contains the cup zone (see Fig.1) .

Let $\overline{\boldsymbol{P}} \subset \mathbb{Z}^2$ (2-dimension Euclidean space of integer number) denote the set of pixel points of the papilla in an original image. It will be recognised by fusion strategy based on the binary images $\boldsymbol{R_b}, \boldsymbol{G_b}, \boldsymbol{T_b}, \boldsymbol{q_1}$ and $\boldsymbol{q_2}$. The main principal of fusion is described as follows:

Let

$$f(x,y)=\alpha_r(x,y)\times R_b(x,y)+\alpha_g(x,y)\times G_b(x,y)+ \alpha_t(x,y)\times T_b(x,y)+q_2(x,y) \quad (4)$$

here $0 \le \alpha_r(x,y)$, $\alpha_g(x,y), \alpha_t(x,y) \le 1$ and they correspond respectively to the normalised intensity values (in [0,1]) of the channels ***R***, ***G***, and ***T***, that are filtered by a maximum filter in order to eliminate the "dark" vessels in region $\overline{q}_2$. The filter size is bigger than the maximum width of vessels in the fundus image. From (4) we can get the binarisation function:

$$P(x,y) = q_1(x,y) \times \chi_{(0,+\infty)}(f(x,y)-\theta) \quad (5)$$

here $\chi_{(0,+\infty)}(x) = \begin{cases} 1, & if \quad x \in (0,+\infty) \\ 0, & if \quad x \notin (0,+\infty) \end{cases}$

and $\theta$ =0.7 determined by statistics. Then the set of pixel points on the papilla, $\overline{P}$, can be got :

$$\overline{P} = \{(x,y) \mid P(x,y) = 1, (x,y) \in I\} \quad (6)$$

The $q_2(x,y)$ in (4) guarantees the region $\overline{q}_2$ to be recognised as a part of the papilla.

Fig.3 shows the image ***a*** in Fig. 1, the papilla detected by the fusion method and the intensity of three channels. In Fig. 4 the fusion procedure is shown for the image ***a***. The other two examples (one with red channel) are shown in Fig. 5

Original image ***a***

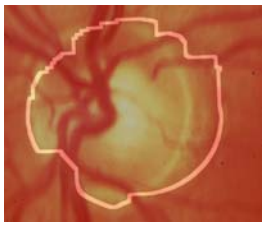

Superposition of the edge ***P(x,y)*** on the image ***a***

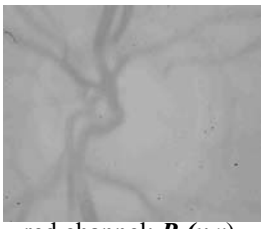

red channel: ***R (x,y)***

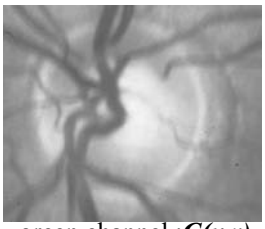

green channel :***G(x,y)***

blue channel: ***R*** (x,y)

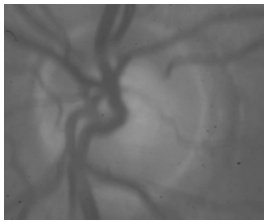

***T(x,y)***

Fig. 3 The papilla detection and channel intensities

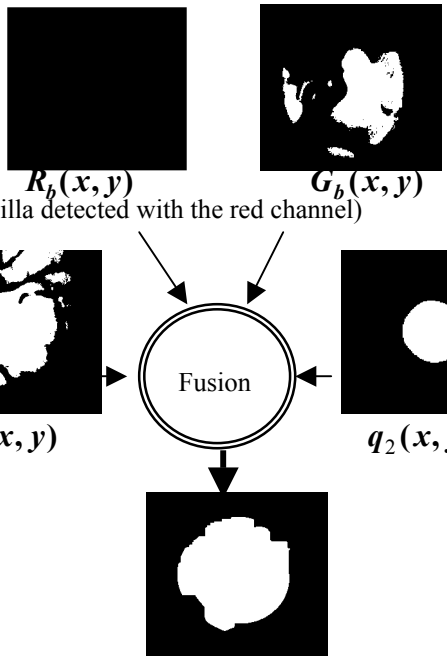


(no papilla detected with the red channel)

The result of fusion: $P(x,y)$ (processed by image filling)

Fig. 4 The procedure of the fusion method for image ***a***

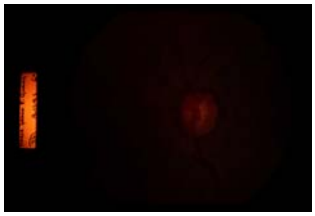

Image ***e*** (low contrast)

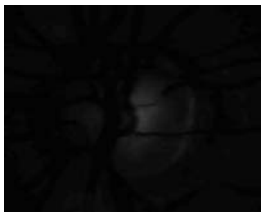

The green channel (a part of image e)

(The green channel of image ***e*** is not effective for papilla recognition)

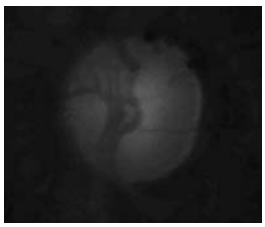

The red channel of image ***e***

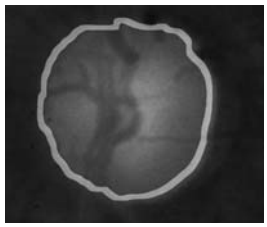

The papilla detection

Image ***f***

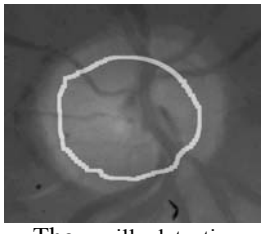

The papilla detection

(Both red and green channels of image ***f*** are effective for papilla recognition)

Fig. 5. Two examples of papilla detection with fusion method

*2.3 Post-processing of papilla shape detected by fusion strategy*

The shapes of the areas detected by the fusion method are sometimes larger or smaller than the papillae (see image ***a*** in Fig. 3 and image ***f*** in Fig. 5). The correction of the shape detected is implemented with an adaptive region growing method. The pixel points in the papilla, that are recognised by the fusion method, are taken as "seed" points. As sometimes the shape detected by fusion method is a little larger than the papilla, the erode transform of mathematical morphology is applied to the pixel point set $\overline{P}$ (see (6)) in order to make the "seed" area smaller than the original papilla area. Thus, a correct implementation of region growing is guaranteed.

For the region growing, a weighted intensity value of a pixel point (x,y) in RGB model is used and defined as follows:

$$WI(x,y)=0.5\times R(x,y)+0.3\times G(x,y)+0.2\times B(x,y) \quad (7)$$

The three coefficients in (7) result from the fact that the red intensity usually reflects the feature of papilla zone (see red channel in Fig.5), the green delivers the features of the papilla boundary and cup (see the green channel in Fig. 3), and the blue is only sometimes effective for the cup zone (see the blue channel in Fig. 3). These coefficients are determined by statistics and will be improved by an adaptive procedure in the future.

The procedure of papilla shape correction by means of the region growing method is described as following:

1) Erode transform on *set* $\overline{P}$ (in (6))

Let ***Sb*** be a rectangular structure element and denoted as a set ***Sb***={(x,y) | (x,y) $\subset \mathbb{Z}^2$ and 0≤x,y≤30 }. The erosion of the set $\overline{P}$ by ***Sb*** is defined as :

$$\overline{P}\ \theta\ Sb=\{(xz,yz) \mid Sb[(xz,yz)]\subseteq \overline{P}, \text{ for } (xz,yz)\subset \mathbb{Z}^2\}$$

here ***Sb***[(xz,yz)]= {(x+xz ,y+yz) | (x,y) $\in$ ***Sb*** }.

2) Region growing [7]

*i)* Initialisation of the seed set :

Let set $rg^{(0)} = \overline{P}\ \theta\ Sb$

ii) Computation of the threshold value for region growing and region growing criteria:

The adaptive threshold value $T_h^{(k)}$ (k=0,1,2…) for region growing is calculated by the intensity means of ***WI***(x,y) and their standard deviations in the seed set $rg^{(k)}$ and ***I*** as follows.

$$m_p^{(k)}=\frac{1}{n_k}\sum_{(x,y)\in rg^{(k)}} WI(x,y) \quad (8)$$

$$m_I^{(k)}=\frac{1}{N}\sum_{(x,y)\in I} WI(x,y) \quad (9)$$

$$\sigma_p^{(k)}=\sqrt{\frac{1}{n_k}\sum_{(x,y)\in rg^{(k)}}(WI(x,y)-m_p^{(k)})^2} \quad (10)$$

$$\sigma_I^{(k)}=\sqrt{\frac{1}{N}\sum_{(x,y)\in I}(WI(x,y)-m_I^{(k)})^2} \quad (11)$$

here ***N*** is the number of pixel points in the image ***I***, and $n_k$ is the number of pixel points in $rg^{(k)}$. The threshold value for region growing is calculated as follows:

$$T_h^{(k)}=(m_p^{(k)}-m_I^{(k)})\times(1+\frac{\sigma_p^{(k)}}{\sigma_I^{(k)}})\times\frac{1+m_I^{(k)}}{1+m_P^{(k)}} \quad (12)$$

In (12) the first right side term $(m_p^{(k)}-m_I^{(k)})$ delivers the difference between the papilla region and the background within an image. The second term depends on the uniformity of the intensity distribution in $rg^{(k)}$. If $\sigma_p^{(k)}\to 0,$ then it tends to 1. It means that a smaller threshold can be used for the region growing due to the uniform distribution of the intensity in $rg^{(k)}$. The third term $\frac{1+m_I^{(k)}}{1+m_P^{(k)}}$ < 1 is used as a weight factor to control over growing (outside of the papilla region) .

$\forall\ (x,\ y)\in I$ and $(x,y)\notin rg^{(k)}$ ,

let $d_c(x,y)=\sqrt{(x-x_c)^2+(y-y_c)^2}$ the distance between (x,y) and $(x_c,y_c)$, and

$$\eta(x,y)=\frac{d_c(x,y)}{\omega}$$

here $\omega$ is the maximum distance from the point $(x_c,y_c)$ to the boundary of ***I.***

If $\left|WI(x,y)-m_p^{(k)}\right|\le T_h^{(k)}\times e^{-\eta(x,y)}$

then

$$rg^{(k+1)}=rg^{(k)}\bigcap(x,y) \quad (13)$$

here $e^{-\eta(x,y)}$ is used to slow down the growing speed as $rg^{(k)}$ grows to the boundary of the image. This step iterates until there is no pixel point left that is recognised in the papilla region.

3) Papilla shape analysis

The papilla area segmented in 2) usually consists of subregions that are not continuous and connected due to the darker areas of the vessels (see appendix). Sometimes, because of noises and exudates, some subregions do not belong to the papilla. The identification of each subregion in the papilla is based on shape analysis and the assumption that a papilla in a fundus image appears as a circle. Therefore, the circle similarity of a region, that consists of a set of subregions recognised, is used to identify each subregion whether it belongs to the papilla. The area (it contains a set of subregions), which has maximum similarity with a circle, is recognised as the papilla area. The similarity of a set of subregions with a circle is calculated as :

$$c_s = \left| 1 - \frac{area}{\pi \times (dist/2)^2} \right| \qquad (14)$$

here ***area*** is the sum of areas of the set of subregions recognised and ***dist*** is the maximum distance of two pixel points within this set. Obviously when $c_s \to 0$, the circle similarity increases. Comparing the papilla recognitions in Fig. 3, Fig. 5 and Fig. 6, we can see that after shape correction with the region growing method the papilla shape recognised is very much improved. Some more examples of papilla recognition with fusion and region growing methods are shown in the appendix

Image ***a*** :

Image ***f***:

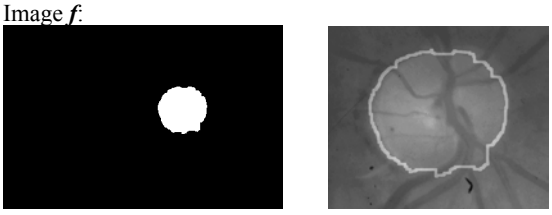

image ***e*** :

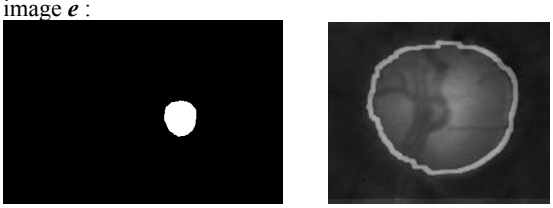

Fig. 6. Shape correction of the papilla recognised by means of the fusion method with region growing. ***On the left***: The shapes of papillae (of images ***a***, ***e*** and ***f*** in Fig.3 and Fig. 5) in the full size images recognised by the fusion method and corrected by region growing. ***On the right***: the superposition of the papilla shapes (denoted as the edges) and the parts of the colour images ***a***, ***f*** and ***e***.

## 3. CONCLUSIONS

The experimental tests with the broad variety of images (see the original fundus images in Fig.1, Fig.2 and the appendix) showed that the fusion method presented in this paper is a very effective method for papilla localisation and shape detection compared to other methods, especially for large size images (4032x2688, 48bit RGB). The limitations of the fusion, that cause the area recognised to be bigger or smaller than the papilla in fundus images because of the three partial results, are improved by the adaptive region growing method. The tests of the methods in this paper on the fundus image database of the European Glaucoma Prevention Study with different exposure conditions and qualities showed that the time consumed and the accuracy rate (94 % from 50 typical images tested) of papilla recognition are fully satisfactory. Some papilla recognitions of these fundus images are shown in the appendix. These methods are used in fundus image registration and 3D reconstruction within the project GlauCAD.

## REFERENCES

[1] J. S. Duncan, N. Ayache, “Medical image analysis: progress over two decades and the challenges ahead”, IEEE Trans. PAMI, 22(1), 85-106, 2000

[2] C. Sinthanayothin, J. F. Boyce, H. L. Cook, T. H. Williamson, "Automated localisation of the optic disc, fovea, and retinalblood vessels from digital colour fundus images” Br J Ophthalmol, 83, 902-910, 1999

[3] A. v. Freyberg, J. Peters, H. Selzer, G. Goch, “Automatic Coutour Detection for Computer Aided Glaucoma Diagnostics”, International Symposium on Photonics in Measurement, June 11-12 2002, Aachen, Germany, 61-68

[4] Y. Wang, B. Lohmann, “Multisensor Image Fusion: Concept, Method and Application”, Science Report in the Institute of Automation Technology at the university of Bremen, 2000. (not published)

[5] S. Tamura, “Zero-crossing interval correction in tracing eye-fundus blood vessels”, Pattern Recognition, 21(3), 227-233, 1988

[6] T. Walter, J. C. Klein, “Segmentation of color fundus images of the human retina: detection of the optic disc and the vascular tree using morphological techniques”, Second International Symposium on Medical Data Analysis (SMDA),October 9-11, 2001, Madrid, Spain.

[7] R. C. Gonzalez and R. E. Woods, “Digital Image Processing”, Second Edition, Prentice Hall, Inc., 613-615, 2002

## ACKNOWLEDGEMENTS

The project GlauCAD (http://www.glaucad.com/) is funded by the European Commission, Fifth (EC) Framework Programme 1998–2002, Specific Programme – ”Quality of Life and Management of Living Resources” (Contract No QLG1–2000–00651).

**Authors:** Yandong Tang, Phone: ++49-421-2185517, e-mail: tan@biba.uni-bremen.de;
Axel von Freyberg, Phone: ++49-421-2185517, e-mail: frb@biba.uni-bremen.de;
Prof. Dr. Horst Selzer, Phone: ++49-421-2185613, e-mail: sz@biba.uni-bremen.de;
Prof. Dr. Gert Goch, Phone: ++49-421-2185515, e-mail: gg@biba.uni-bremen.de;
Bremer Institut für Betriebstechnik und angewandte Arbeitswissenschaft an der Universität Bremen, Hochschulring 20, 28359 Bremen, Deutschland, Fax: ++49-421-2185625

## APPENDIX

Example 1.

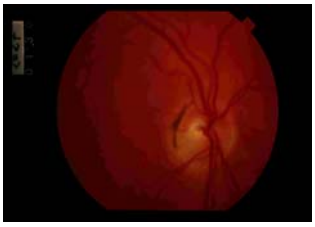


Original image ***g*** (on the left side) and the shape of the papilla (on the right side) in image ***g*** recognised by the fusion and region growing methods.


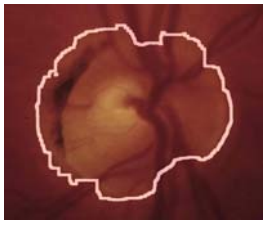

***On the left side*****:** The papilla shape recognised in image ***g***. ***On the right side:*** superposition of the papilla edge generated from the papilla shape on the original image ***g*** (only the region around the papilla is shown).

Example 2:

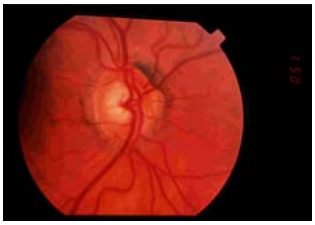
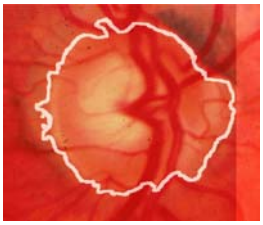

***On the left side:*** the original image ***h***. ***On the right side***: superposition of the papilla edge recognised on the original image ***h*** (only the region around the papilla is shown).

Example 3 :

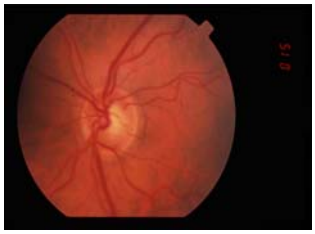


***On the left side:*** the original image ***i***. ***On the right side***: superposition of the papilla edge recognised on the original image ***i*** (only the region around the papilla is shown).

Example 4:

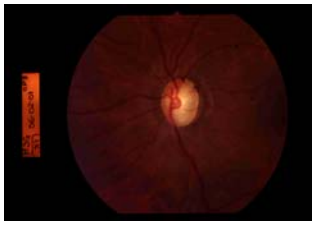


***On the left side:*** the original image ***j***. ***On the right side***: superposition of the papilla edge recognised on the original image ***j*** (only the region around the papilla is shown).

Example 5:

The original image ***k***: The papilla in the image was not correctly recognised, because the papilla centre was localised wrong due to the “brighter“ and yellowish region on the top right.